ASSESSING FEMUR AND PELVIS INJURY RISK IN CAR-PEDESTRIAN COLLISIONS: COMPARISON OF FULL BODY PMTO IMPACTS, AND A HUMAN BODY FINITE ELEMENT MODEL

Jess G. Snedeker
Felix H. Walz
Markus H. Muser
Christian Lanz
Working Group on Accident Mechanics, Institute of Biomedical Engineering, University and Swiss Federal Institute of Technology, Zurich
Switzerland
Günter Schroeder
Institute of Legal Medicine, Hanover Medical School
Germany
Paper number 05-103

ABSTRACT

A considerable potential for reducing fatalities of pedestrians and other vulnerable road users lies in the design of car front shapes. Vehicle safety tests have been proposed by the EEVC WG17, and are currently in discussion by legal entities, as well as car makers.

In this study, we first present numerical simulations of various pedestrian impacts against several different simplified hood shapes. Impacts were simulated using a detailed finite element model of a mid-size pedestrian that has been extensively validated in previous studies. As expected, the model revealed that biomechanical loading patterns are heavily influenced by hood leading edge shape.

In a second step, femoral and pelvic bone surface strains were measured in five full body PMTO impacts at 40 kph using physical representations of the simulated car shapes. Each PMTO was instrumented with strain gauges on the impact side: four on the femoral shaft, three on the femoral neck, and three on the superior ramus of the pelvis. Accelerometers were placed on the dorsal aspect of vertebra T6 and L5. High speed digital video was recorded at 1,000 frames per second from the side. Fracture risk was examined with respect to car geometry, pedestrian stature, and bone quality as indicated by peripheral quantitative computed tomography (pQCT) of the femoral neck.

Experimental results indicated a remarkable predictive ability of the finite element model in assessing femur and pelvic injury risk. Strain data yielded valuable insight into the failure threshold of the pelvic rami, which was observed to fracture in three of the tests. The largest factor in pelvic fracture was low bone quality, rather than car geometry. Based upon results of the model and PMTO experiments, recommendations are offered for a more appropriate characterization of the hood shape with regard to pelvis and femur injury risk.

INTRODUCTION

Pedestrians and bicyclists represent an extremely vulnerable population of road users, and thousands are severely injured or killed every year. It has been reported that upper leg and pelvis injury occur in just over 10% of pedestrian-vehicle impacts (Matsui et al., 1998). Vehicle-pedestrian crashes are responsible for 10% to 20% of all adult pelvic fractures and 60% to 80% of pediatric pelvic fractures (Sheppard, 2001).

The intelligent design of automotive front-end geometry holds a large potential for reducing injuries in unprotected road users. In order to assess the risk posed to a pedestrian by an automobile, the European Experimental Vehicles Committee (EEVC) has proposed three subsystem pedestrian dummy tests (EEVC Working Group 17, 1998). These tests represent a significant investment of the limited resources available for pedestrian protection. For such tests to be useful, it is essential to concentrate on the most relevant aspects of automotive design, and

employ testing protocols that are capable of successfully identifying high-risk vehicles. This study focuses on the upper leg (UL) impact portion of the EEVC protocol, which is intended to assess the risk of femur and pelvis injury in a struck pedestrian.

Vehicle front end geometry plays a critical part in the resulting kinematics of pelvic/upper leg impact. The EEVC prescribes a systematic method for characterizing the front end geometry of an automobile. With regard to the UL subsystem test protocol, three geometric parameters are considered:

1) Upper Bumper Edge Height (BH) – The upper limit to significant points of pedestrian contact with the bumper. It is defined as the vertical distance between the ground, and the upper-most point of contact between a 700 mm long reference line and the bumper when the line is inclined rearwards by 20 degrees, and traversed across the car front at ground level.

2) Hood Leading Edge Height (LEH) – Defined as the point of contact between a reference line 1000 mm long and the front surface of the hood when the line is inclined rearwards by 50°, with the lower end 600 mm above ground.

3) Bumper Lead (BL) – is the horizontal distance between the upper bumper reference line and the hood leading edge reference line.

The EEVC WG17 test protocol employs these characteristics within a system of look-up tables based on kinematic analysis of cadaver and dummy impact experiments. The look-up tables are intended to incorporate pedestrian impact kinematics into the UL testing protocol. Previous studies have identified an apparent discrepancy between injury risk as assessed by the EEVC UL test protocol, and real-world accident experience (Matsui et al. 1998, Konosu et al. 1998, EEVC WG17 1998, Konosu et al., 2001, Okamota et al. 2001, Snedeker et al., 2003). This discrepancy has been primarily attributed to the simplification of the complicated three dimensional kinematics of vehicle-pedestrian impact, to a one dimensional impact test.

The current study examines the possibility that this discrepancy also arises from an inadequate characterization of vehicular front end geometry. The geometric characteristics that play a critical role in pedestrian impact are examined with the goal of identifying potentially important considerations that are neglected or improperly accounted by the current version of the EEVC protocol.

METHODS

In this study, we first performed numerical simulations of various pedestrian impacts against different simplified hood shapes. Impacts were simulated using a detailed finite element (FE) model of a mid-size pedestrian (THUMS) that has been extensively validated against PMTO experiments in previous studies (Iwamoto et al., 2002) and specifically validated for use in the study of pedestrian impact (Snedeker et al. 2003).

In a second step, measurements of femoral and pelvic cortical bone surface strains were recorded in five full body PMTO impacts at 40 kph against physical representations of the simplified car shapes used in the FE simulations. Each PMTO was instrumented with strain gauges on the impact side femur and pelvis, as well as with accelerometers on the dorsal aspect of the spine. The results from the impact tests were then compared with the corresponding simulations.

Finally, insights obtained from the first two steps were used to critically reexamine the EEVC UL test protocol. Specifically, an attempt was made to redefine the important aspects of car geometry, and implement them into a revised protocol.

<u>Creation of the simplified automotive geometries</u>

Fifteen simplified automotive car shapes were created for FE simulation of pedestrian impact. The car geometries were equally divided among three classes: Sedans, SUVs, and Vans/One-Box. Five to six actual production vehicles from each class were individually measured to produce a geometric template for the class. The geometric parameters used to create each template are illustrated in Figure 1. Class average and standard deviations for each class are listed in Table 1.

Within each class, five geometries were created by varying the radius of the hood leading edge, while keeping all other parameters constant. Radii of 0, 50, 100, 250 and 500 mm were created. Thus within a given class, all geometries had identical bumper height, bumper width, bumper lead, leading edge height, hood pitch, and windscreen position, but differing hood leading edge roundedness.

In the FE simulations, each automotive geometry was modeled using a total of 1,000 quadratic shell elements. The front end was represented by a 0.8 mm thick sheet metal (ASTM-A36) hood supported with a stiff steel frame. The bumper was modeled as 2 mm thick ASTM-A36 steel plate covered by a 50 mm thick hard PVC shell. A plastic hardening function

was employed to represent the yield behavior of steel. Thicknesses of the hood sheet metal and bumper materials were set to accord with realistic deformations as reported in the literature (Matsui et al., 1998, Ishikawa et al., 1993, Bunketorp et al. 1983).
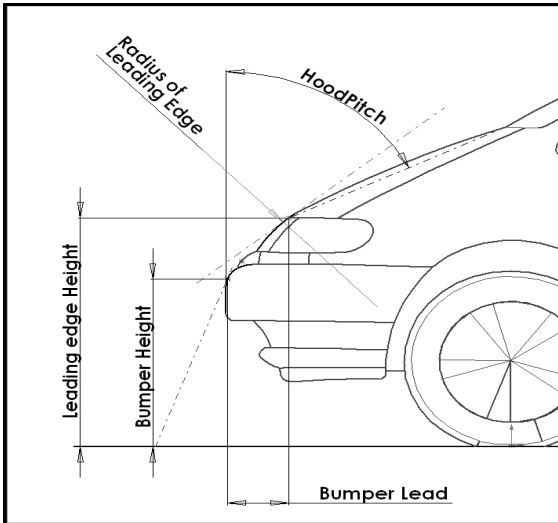
**Figure 1. The geometric characteristics used to create each automotive class temp**

Table 1. Average measurements (lengths in mm; angles in degrees) and standard deviations for the geometric parameters used to create an automotive class template.

	Sedan		SUV		Van / A-Box	
	Class Avg.	STD	Class Avg.	STD	Class Avg.	STD
Model Year	1996	2.9	1998	1.4	1997	1.7
BH	500	20	640	30	580	60
BL	140	20	140	50	160	60
LEH	740	50	1020	90	860	130
Rad. LE	230	130	410	370	730	530
Hood Pitch	79	1.5	80	2.9	65	4.5

Pedestrian impact finite element simulation

The FE model used to simulate pedestrian impact was the Total Human Model for Safety (THUMS), provided by Toyota Central R&D Lab., Inc., and implemented within the PAM-Crash® v2001 FE software. The THUMS model consisted of nearly 85,000 elements, and over 1,000 separate material models. In addition to bone structures and soft tissues, the model included relevant muscles, ligaments, and tendons. For specific information on

the construction of the human FE model, the car geometry FE models, and the validation of the THUMS femur and pelvis for use in simulating femur and pelvic injury, the reader is referred to Snedeker et al., 2003.
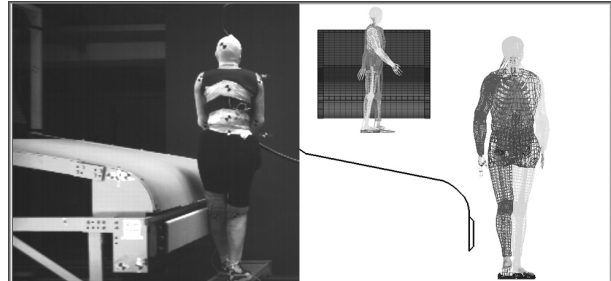
Figure 2. Simplified vehicle geometries were constructed for actual PMTO impacts (left). The vehicles were constructed according to the specifications used in FE simulations (right).

In each simulation, the THUMS model was permitted to settle under the load of gravity such that each leg supported 50% body weight at the time of impact. The foot/ground coefficient of friction was set at 0.65. The coefficient of friction between the car surfaces and impacted body parts was set at 0.25. The initial velocity of the car was 40 kph (11.1 m/s) at time of impact, and the car was decelerated at 6.9 m/s^2, to replicate braking by the driver.

Construction of the PMTO impact vehicle geometries

In the PMTO impacts, four vehicle fronts were constructed according to the same physical specification as used in the FE simulations. The sheet metal thickness was adjusted until force deflection characteristics matched those of the FE model. The geometries constructed for the PMTO tests consisted of: a sedan with a 50 mm radius hood leading edge (Sed050), a sedan with a 250 mm radius hood leading edge (Sed250), a van with a 50 mm radius hood leading edge (Van050), and a van with a 250 mm radius hood leading edge (Van250).

PMTO impact experiments

All PMTO tests were performed in accordance with German federal and local laws regarding the use of human test subjects. Cadavers were obtained from the Medical University of Hanover anatomy department.

As indicated in Table 2, the PMTOs varied in age, sex and stature. Test subjects were excluded from the study for pre-existing bone fractures of the legs and pelvis, as indicated by diagnostic radiograph

3

images. Each PMTO was instrumented with ten strain gauges (*Vishay Micro-Measurements, Inc., Raleigh, NC, USA*) to measure cortical bone surface strains. Strain gauges were applied using well established techniques (Cordey, 1998). Briefly, the periosteum was scraped away using a scalpel blade and surgeon's rasp, the gauging area was cleaned with a chemical solvent to remove lipid contaminants, and a combination activator-cyanoacrylate bonding agent was applied to the back of the gauge before mounting.

Table 2. PMTO specifications

ID	Sex	Age	Height (cm)	Mass (kg)
T1	F	52	160	50
T2	F	76	166	74
T3	M	32	177	75
T4	M	78	180	64
T5	M	76	172	60

An anterior, inverted - "L" shaped incision was made from the left knee to the hip, and then from the hip to the pubic symphysis. Care was taken to minimize disruption of ligaments and tendons; however, access to the femoral neck required partial dissection of the hip joint. It should be noted here that no hip dislocations were observed in post-impact autopsy. A single axis strain gauge was centered on the midpoint of the lateral aspect of the femoral shaft, with the principal axis of the gauge aligned with the long axis of the bone. A strain gauge rosette was placed on the medial aspect of the femur, with the axis of the center gauge aligned with the long axis of the bone. A second strain gauge rosette was placed on the inferior/anterior aspect of the femoral neck, and another on the superior/anterior aspect of the superior ramus of the pelvis. All gauges were placed on the left (impact) side of the PMTO according to Figure 3. Location of the strain gauges necessarily varied between subjects due to anatomical differences in bone geometry and obstruction of the gauge installation site by tendon and ligament insertions.

Strain gauges were excited in a quarter-bridge configuration using a DC-amplifier and signal conditioner (*Vishay model 2100, Vishay Micro-Measurements, Inc., Raleigh, NC, USA*). Output signals were digitized and recorded using a 16 bit

analog/digital data acquisition system (*Labview v7.0 and NI DAQCard-6036E, National Instruments Corporation, Austin TX, USA*). Triaxial accelerometers (*Endevco Corporation, San Juan Capistrano, CA, USA*) were screwed into the dorsal aspect of vertebrae T6, and vertebrae L5.
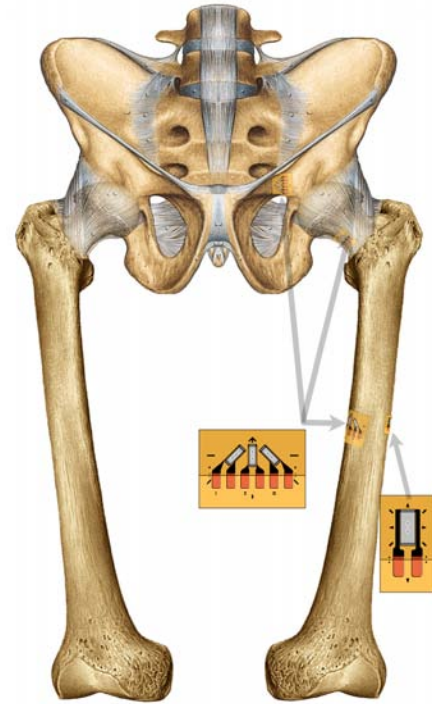
Figure 3. Strain gauge placement (Anatomy adapted from Sabotta, 1993)

Prior to impact, the PMTO was positioned in the stance phase of gait, with the left foot forward. To prevent the arms from obstructing contact with the car front, the hands were bound at the wrist in front of the subject. At 65 ms prior to impact, the subject was released from an overhead support using an electro-mechanical switch. The PMTO was thus permitted to settle under the load of gravity for 65 ms before being impacted from the left side.

For each PMTO, one of the four automotive geometries described above was bolted to the test sled. The initial velocity of the sled was 40.0 ± 0.3 kph at time of impact, and the sled was decelerated at 13 m/s^2 after contact. Details about the impact conditions of each test are listed in Table 3. Impact and post-impact kinematics were recorded at 1,000 frames per second from two high speed digital video cameras mounted perpendicularly to the sled track. A lateral view of the car geometries and relative statures of the PMTOs is shown in Figure 4.

4

Table 3. The LEH/Hip ratio gives an indication of the hood edge contact point on the leg. For example, in the case of 100%, the hood edge strikes the greater trochanter. A ratio of 75% would correspond roughly to contact with the midshaft of the femur.

PMTO	Geometry	Impact Speed	Ratio LEH to Hip height
T1	Sedan 250	40.1	97%
T2	Sedan 250	40.0	91%
T3	Sedan 050	40.0	83%
T4	Van 050	39.8	96%
T5	Van 250	39.7	100%

Figure 4. While geometries for a given vehicle class have identical hood edge height as defined by the current EEVC protocol, the effective hood leading edge height is higher with respect to smaller stature pedestrians.

After impact, diagnostic radiographs were made of the struck-side femur, tibia/fibula, knee joint, hip joint, and pelvis. The body was then autopsied by a qualified forensic medical doctor, and impact-related injuries were catalogued. Sections of bone specimens were removed at the strain gauge location, and were assessed for bone quality using a peripheral quantitative computer tomography (pQCT, *Scanco Medical, Bassersdorf, Switzerland*). The pQCT scans

with a spatial resolution 90 µm were analyzed for cortical and trabecular bone architecture, and were assessed with regard to osteoporosis. According to World Health Organization standards, subjects with bone quality more than 1 standard deviation below average of a healthy population are considered "low-bone" and subjects more than 2.5 standard deviations below are clinically diagnosed as having osteoporosis. It should be noted that pQCT provides vastly superior spatial resolution over two-dimensional diagnostic techniques, and provides the capability to analyze bone structure geometrically. However, baseline data-sets published in the literature are limited. The baseline dataset (n=60) used in this study comes from Hirokoshi et al., 1999.

Data analysis

Raw strain gauge data were filtered using a low-pass CFC-600 filter, and converted to strain data using the calibration gauge factors provided by the manufacturer. Bone stresses and bending moments were calculated by multiplying strain by an assumed elastic modulus of 17 GPa (McElhaney, 1966). Bending moments at the femur were calculated using classical beam theory:

$$M = \frac{\varepsilon * E * I}{r_o} \quad \text{where,} \quad I = \frac{\pi}{4}\left[r_o^4 - r_i^4\right],$$

ε is measured strain, E is the elastic modulus, I is the moment of inertia for a hollow cylinder, and r_i and r_o are mean femoral midshaft internal and external radii, respectively. The midshaft radii were obtained during autopsy by averaging five measurements of periosteal shaft diameter and cortical wall thickness.

Kinematic analysis of the high-speed video was performed to assess the danger presented to the pedestrian for a head first secondary impact with the road. A qualitative comparison between the kinematics of the FE model and those of the PMTOs was also performed. Video was further analyzed to estimate the closing speed of contact between the car hood leading edge and the leg or pelvis of the PMTO. Finally, the measured bone strains, bone stresses, and observed injuries were analyzed with respect to car geometry and bone quality as assessed by pQCT.

Proposed Modifications to the EEVC Upper-leg Testing Protocol

An attempt to improve the current EEVC UL impact protocol was made via a modification of the test conditions. It was hoped to increase bio-fidelity of the test protocol with minimal changes to the

impactor itself. Modifications of impact velocity, impactor mass, impact angle, and impact height (leading edge height) were based on simplified geometric/anatomical principles and observations from both the FE simulations and PMTO experiments. Madymo® simulations employing the proposed protocol changes were then compared against the default EEVC conditions, the results of the FE model, and the PMTO impact results.

RESULTS

Bone fracture, and other injuries: Simulation vs. PMTO experiments

Three PMTO fractures of the struck-side superior ramus were observed, including the sedan 250 (T2) and both van geometries (T4 and T5). Fractures of the acetabulum were also observed in both van impacts (T4 and T5). FE simulation predicted pelvic fractures for only the small radius van geometry (Van050). Acetabular fractures were not predicted by the THUMS for any car/van geometry. No PMTO femoral fractures were observed, nor were they predicted by the FE simulations for any of the test geometries. Fractures of the lower legs were not analyzed using the model.

Kinematic analysis revealed a straightforward mechanism of pelvic loading when impacted by high leading edge geometry (LEH $\geq$ hip height); the hood leading edge contacted the femur at or above the greater trochanter, loading the pelvis obliquely through the axis of the femoral neck (the PMTO pelvis was rotated 20 degrees (cw) in the coronal plane with respect to the impact direction). However, for automotive geometries with hood leading edges lower than the hip, the soft tissues of the thigh make first contact, and the loading path to pelvic structures is considerably more complicated.

Only PMTO T3 (a 50th% man impacted by Sed050) was clearly a case of leading edge contact with the midshaft of the femur. This can be seen qualitatively in Figure 4 above, and quantitatively in Table 3 as the ratio of LEH/hip-height. The other PMTO trials, including PMTO T2 (impacted by Sed250), were to a much greater extent impacted at the proximal femur and pelvis.

Bone quality measured by pQCT

To investigate the possible influence of bone quality on the observed fracture patterns, the femoral necks of all five PMTOs were scanned using pQCT (Table 4, Figure 5) and analyzed for bone quality.

Consistent with their age group. subjects T1 and T3 had healthy trabecular bone, cortical bone, and overall total bone quality, while subjects T2, T4 and T5, had poorer trabecular density, trabecular connectivity, cortical bone density, and lower overall bone density.

Table 4. PMTO bone quality and geometry (* = low bone, ** = Osteoporosis). The bone mineral density of the PMTOs in terms of trabecular, cortical, and overall bone mineral density are normalized to values from Horikoshi et al, 1999.

PMTO ID	Trabecular Bone (Z-Score)	Cortical Bone (Z-Score)	Total Bone (Z-Score)	Fem Shaft OD mm	Fem Shaft thick mm	Fem Neck OD mm	S. Ramus OD mm
T1	0.3	1.5	0.9	24	6	22	12
T2	-2.8**	4.2	0.1	29	7.5	28.5	13.5
T3	6.0	2.7	2.8	31	7	31.5	14.5
T4	-1.2	-5.5**	-1.9*	30	7	39	21
T5	-3.9**	2.2	-1.7*	32	7	36	N/A

The observed fractures corresponded heavily to relative bone quality of the PMTO, with all pelvic and acetabular fractures occurring in the lowest bone quality subjects. Thus analysis of the resulting injuries with respect to car geometry, age, and bone quality shows that bone quality seems to be a major factor for a pelvic/acetabulum fracture (Table 5). It also appears that acetabulum fracture is more likely with a high leading edge, such as present on the van geometries. Finally, femur fracture did not occur for any hood leading edge shape, regardless of bone quality. It should be noted, that the large bumper lead of the tested geometries may have helped prevent femur fracture for even sharp hood edges.

Loading mechanism of the femur in lateral pedestrian impact: Finite element results

In the simulations, the automotive front-end geometry had a large effect on the nature of the bending stresses in the femur. In the case of the sedan, the relatively low hood leading edge (745 mm) and moderate bumper lead (150 mm) delays the first contact of the thigh with the hood. This permits the pelvis and proximal femur to accelerate before first contact, thus reducing the closing speed between the thigh and the hood leading edge to between 1 and 6 m/s, depending on the hood leading edge radius.   In
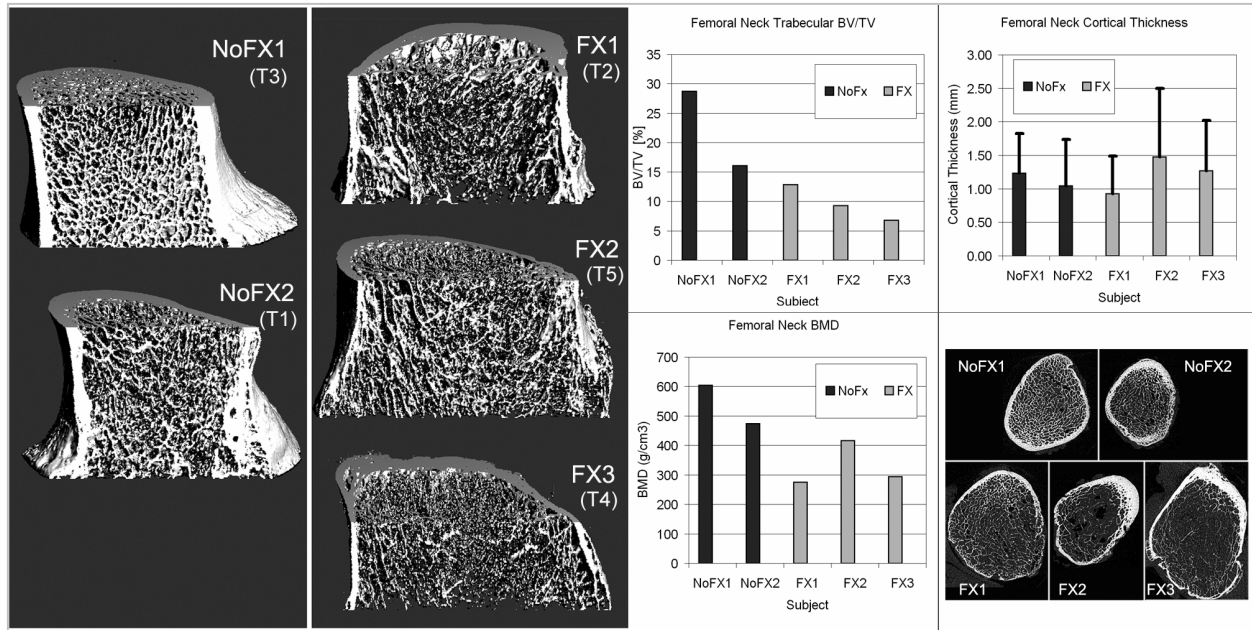
Figure 5. Bone quality was assessed using pQCT scans of the femoral neck.

Table 5. Lower extremity injury related to car geometry, age, pedestrian stature, bone quality.

	Sedan	Sedan	Sedan	Van	Van
Trial	T3	T1	T2	T5	T4
Hood Radius	50 mm	250 mm	250mm	250 mm	50 mm
Age	35	52	76	76	78
Hood Height (% of Hip Height)	83%	97%	91%	100%	96%
Bone Quality	Good	Good	Poor	Poor	Poor
Lower Leg Fracture	No	Yes	Yes	Yes	Yes
Pelvic Ramus Fracture	No	No	Yes	Yes	Yes
Pelvic Acetabulum Fracture	No	No	No	Yes	Yes
Femur Shaft Fracture	No	No	No	No	No

the case of the van/one-box construction (or a sedan with high LEH and/or short BL), the pelvis and proximal thigh do not considerably accelerate before contact with the hood leading edge. Hence, the contact closing velocity is much higher than that of the sedan, and the bending induced by this contact is more severe. In car geometries that involve a hood leading edge lower than the height of the hip, it appears that the bending of the femur, and consequently the associated risk of fracture, are directly related to the closing speed of contact between the thigh and the hood leading edge (Figure 6). According to the model (and verified by the PMTO tests), the roundness of the hood leading edge imparts a rolling motion to the thigh, which reduces the closing speed of contact.

Loading of the femur in lateral pedestrian impact: PMTO results

In general, the mechanism of femoral loading and the corresponding femur shaft cortical strains and bending moments (both magnitude and time history) in the PMTO femur corresponded very well to those predicted by the THUMS model (Figures 7 and 8). However decrepencies arose due to differences in stature between the THUMS and the PMTOs. In tests T1 and T5, the small stature of the subject with respect to the hood edge causes the hip to be

contacted by the hood before the femoral bending moment (and stresses) can fully develop. With respect to hip height, Trials T1 and T5 are more similar to an SUV type impact on a 50th% man, for which the hood edge engages the hip/pelvis at or above the greater trochanter.

In no case was femoral fracture observed. Consistent with this observation, peak recorded femoral shaft cortical bone strain never approached the 2500 $\mu\varepsilon$ threshold associated with fracture (McElhaney, 1966). The measured bone strains and corresponding bending moments of the first peak tend to be less than those predicted by the THUMS model. This may indicate that the THUMS knee is more rigid than that of the PMTO, where skeletal tissues tend to dissipate or absorb impact energy
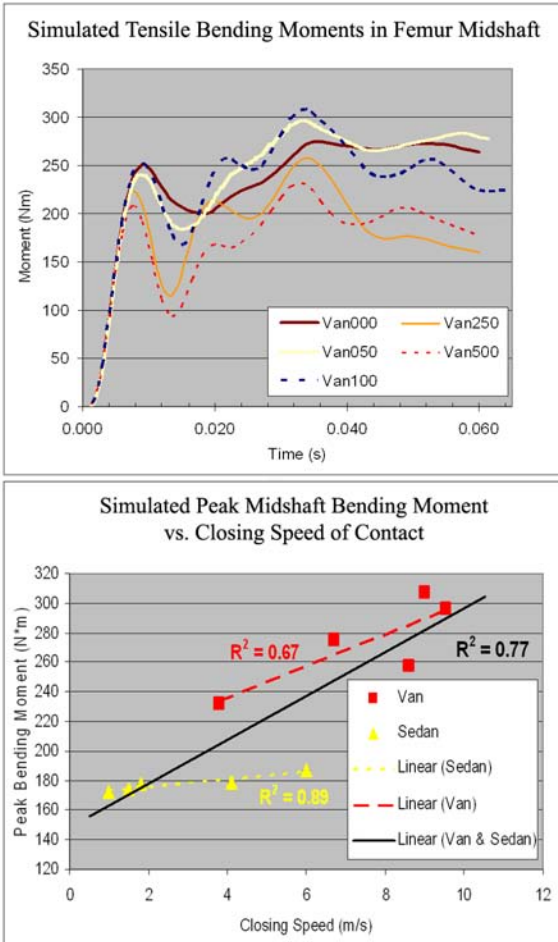

Figure 6. (*Top*) **The larger leading edge radii impart a rolling motion to the thigh. This effectively reduces the closing velocity, and consequently, the peak bending moment in the femur.** (*Bottom*) **As closing speed increases, so does the bending load applied to the femoral shaft due to hood contact. These trends were also observed in the PMTO experiments.**
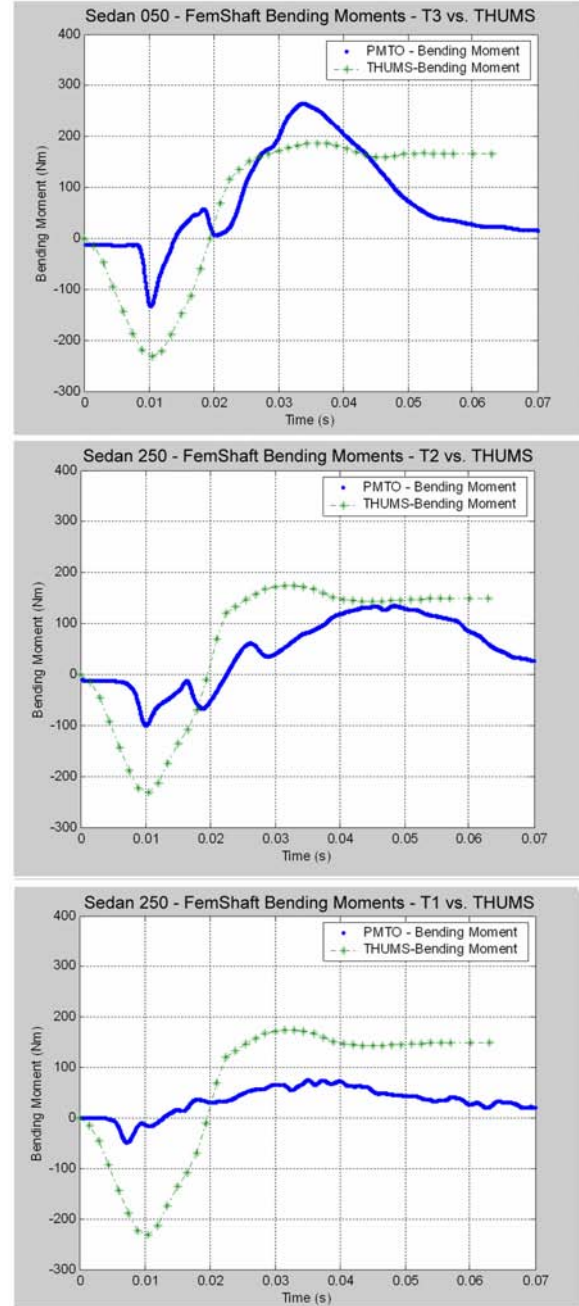

Figure 7. The bending moment in the medial femoral shaft impacted against the sedan. (Top) In PMTO T3, the stature of the subject is very similar to the THUMS. Accordingly, there is particularly good agreement between the experimentally measured bending moments and those predicted by the THUMS model. In PMTO T2 (Middle) and T1(Bottom), the smaller stature of the subject causes hip contact with the hood before the bending moment can fully develop. With respect to hip height, trial T1 is more similar to a van/SUV type impact on a 50th% man. A resulting fracture of the superior pubic ramus in T2 may have also influenced the resulting loads.

8
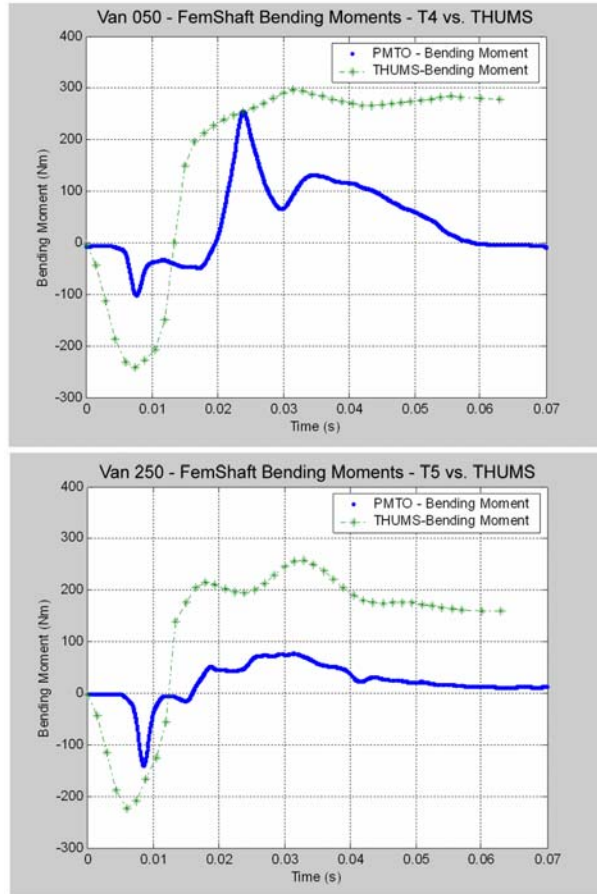
Figure 8. In both van impacts, a catastrophic failure of the acetabulum and superior pubic ramus on the struck side of the PMTO may have contributed to decreased loading of the femur.
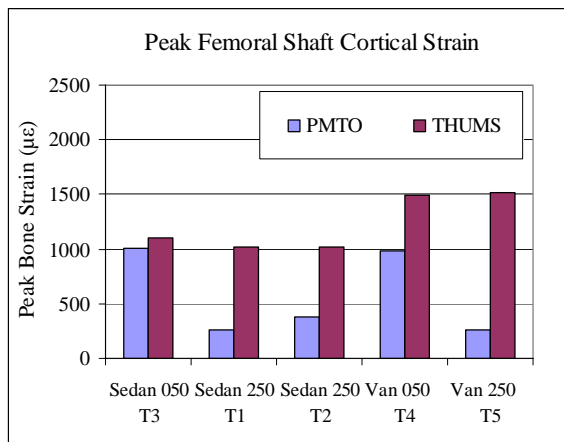
Figure 9. Summary of peak femoral shaft cortical bone strain for the PMTO test series and the corresponding THUMS simulations. Peak tensile strains are less than thresholds associated with tensile fracture (2500 µε), consistent with no observed femoral fractures.

Loading of the pubic ramus in lateral pedestrian impact

The recorded pubic rami strains were similar for all PMTO's (Figure 10). Bone strain increased rapidly after contact between the thigh/buttocks and the hood, then either dropped immediately in the case of pelvic fracture, or continued to rise and then gradually decrease in cases of non-fracture.

The measured peak stress magnitudes in the PMTO pubic rami are consistent with those predicted by the THUMS model (Figure 11). The fracture of the strain-gauged pubic rami observed in PMTO T2, T4, and T5 provide insight into the failure behavior of this structure. Analysis of bone quality by pQCT shows that the discrepancy between the ultimate strains of the fracture cases and the non-fracture cases is most likely due to differences in bone quality (age-related osteoporosis).

Loading of the femoral neck in lateral pedestrian impact

Surgical access to the femoral neck was hindered by the ligaments at the hip. Generally the strain gauges were placed on the inferior/anterior aspect of the femoral neck. Since the gauge placement was variable between trials, the direct comparison of PMTO and FE model femoral neck stresses is complicated.

As can be seen in Figure 12, a prominent peak in the stress vs. time curves can be seen in T2, T4, and T5 at approximately 20 ms after impact. Video analysis indicated that this peak coincided with contact between the hip and hood leading edge.

Analysis of high-speed video: secondary road impact

Video analysis revealed that all PMTOs were rotated between 190 and 270 degrees in the sagital plane depending upon the shape of the vehicular hood. The pedestrians struck by the sedan geometries often made a secondary impact with the hood before landing on the ground. This secondary impact provided additional rotation of the body, and prevented the PMTO from landing head-first on the test track. The shorter, angled hoods of the van geometries, and head contact with the van windscreen caused PMTOs T4 and T5 to rotate approximately 190 degrees, thus resulting in a head-first contact with the ground (Figure 13). It should be noted that PMTO T4 had a cranial fracture, and PMTO T4 and T5 both experienced cervical spine fractures at C7. However, it is not clear whether these injuries occurred as a result of primary, or secondary impact.
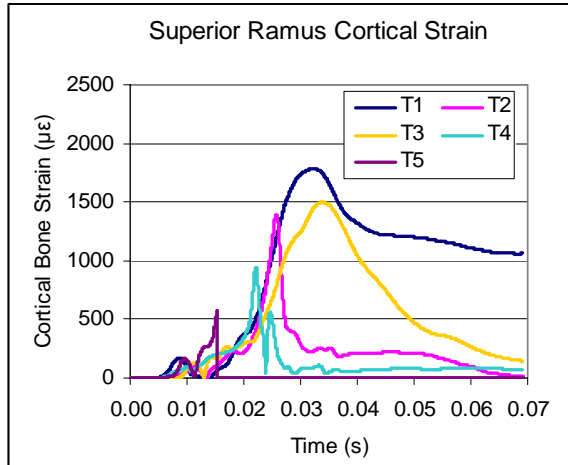
Figure 10. Cortical bone stresses in the superior pubic ramus. Pelvises of T2, T4, and T5 were fractured during impact, as indicated by the sharp drop in strain.
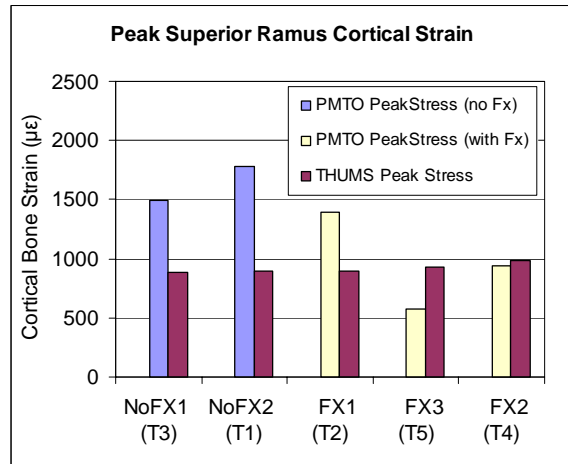
Figure 11. Peak superior pubic ramus tensile cortical strain for the PMTO and THUMS simulations.
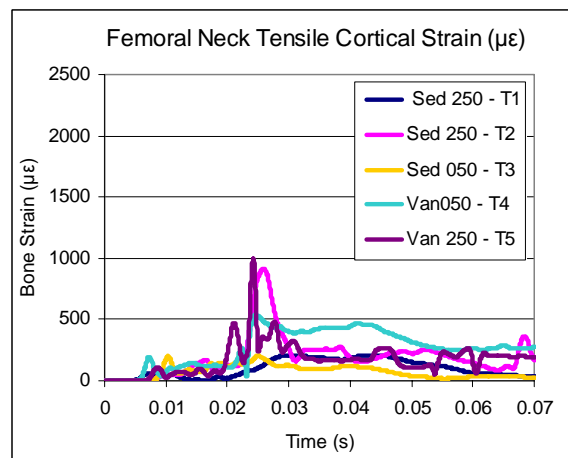
Figure 12. Cortical bone strains in the femoral neck.

Figure 13. Secondary road impact is an very important design consideration that is often neglected. PMTOs struck by the sedan landed on their sides. PMTOs struck by the vans were thrown onto their heads. Notice the use of ground padding cushioned secondary impact, possibly resulting in fewer injuries than would be observed against a rigid road surface.

Proposed Modifications to the EEVC Upper-leg Testing Protocol

Observations from the THUMS simulations and PMTO experiments indicate that EEVC designated hood leading edge is often not the first point of contact with the pedestrian P/UL. The proposed changes to the method of geometric characterization define the hood leading edge height using a "wrap around" contact definition method similar to that already employed for the EEVC headform test protocol. In the proposed modification, hood leading edge height is defined as the first point of contact between the hood and a 1,000 mm long string rotated from the EEVC upper bumper reference line. The impact angle is defined as the angle between the string and the vertical plane (Figure 14).

Results from the present study show that for hood leading edge heights exceeding approximately **90 cm** (defined as per the modified method), the threat of fracture posed to the femur is reduced, and the likelihood that a pelvic fracture will occur is raised. Thus, this LEH threshold is proposed as a transition from test conditions and failure criteria suited to the femur to conditions appropriate for assessing pelvic fracture risk. The test conditions for each of these cases are outlined below in Table 7. The impact tests are executed in exactly the same manner, regardless of whether the pelvis is being tested, or the femur. The difference lies in the selection of the impactor mass, and the pass/failure criteria applied when analyzing the test results.

In particular, the current EEVC UL test protocol fails to reflect the true closing speed of contact between the pedestrian UL and the hood leading edge. This inaccuracy is especially important since impact energy (a critical value with regard to injury likelihood) varies quadratically with impact velocity. With certain velocity assumptions (Figure 14), the closing contact velocity (normal to the long axis of the femur) is a simple geometric relationship. The proposed method uses this geometrical relationship for determining a more appropriate impactor velocity. The selection of the impactor mass is based upon the mass of the involved body segments. For a 50% male pedestrian, the mass of the upper leg (thigh) is approximately 7.5 kg. This is the mass then designated for impact tests of vehicles with a LEH ≤ 90 cm. The 11.1 kg mass for LEH > 90 cm, corresponds to the mass of the 50% male pelvis plus 10% of the upper leg mass. It should be noted that an impact mass of 7.5kg is 2kg less than the default weight of the current EEVC UL impactor. Thus for testing geometries with LEH ≤ 90 cm, modification to the default impactor will be necessary.

The impactor trajectory should follow the measured impact angle along a path such that the impactor shaft centerline coincides with the newly defined leading edge height (Figure 15). Unlike the current version of the EEVC UL protocol, the impact angle and the point of first contact between the impactor and the car front is roughly the same as the actual pedestrian impact.

The proposed test pass/failure criteria (Table 7) are based upon the following observations:
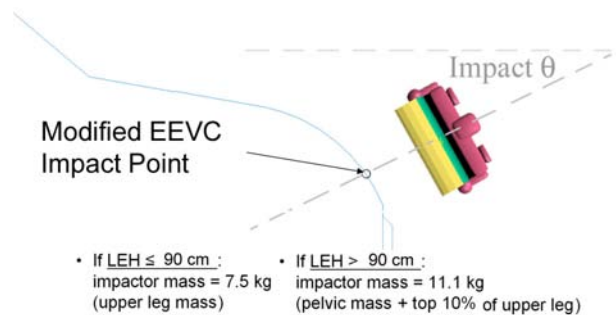
1) The femoral shaft is likely to fail in lateral impact due to stress induced by bending moments. A nominal threshold of 320Nm is suggested based upon quasi static tests of Yamada (1971), and dynamic tests of Powell et
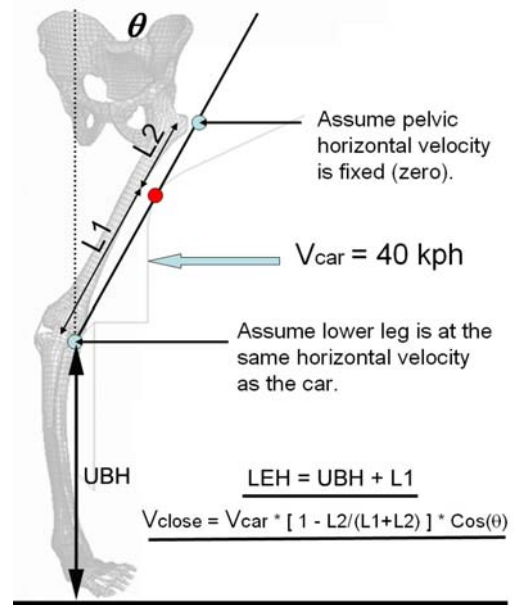
Figure 14. The proposed method for determining the EEVC leading edge height.

$$LEH = UBH + L1$$
$$V_{close} = V_{car} * [1 - L2/(L1+L2)] * Cos(\theta)$$

Table 7. Description of differences in pelvic vs. femur UL test

Region	LEH (cm)	Impact Mass	Failure Criteria
Femur	≤ 90	7.5 kg	Average Bending Moment > 320 Nm (Yamada 1971, Powell et al. 1975, Kress et al. 2001,)
Pelvis	> 90	11.1 kg	Peak Average Force > 10 kN (Cesari 1982)

- If LEH ≤ 90 cm : impactor mass = 7.5 kg (upper leg mass)
- If LEH > 90 cm : impactor mass = 11.1 kg (pelvic mass + top 10% of upper leg)

Figure 15. The impactor is directed along a trajectory such that the impactor centerline is aligned with the Mod-EEVC LEH reference point. Impact masses are determined by the mass of the involved body segments. The test impact mass values are derived from the anthropometric study of Roebuck et al. 1975.

al. (1975) and Kress et al. (2001). Peak bending moments observed in the present PMTO study also suggest that this threshold is reasonable.

2) To our knowledge, no comprehensive data set exists for injury tolerance of the femoral neck and greater trochanter under lateral impact loading.

3) The PMHS studies of Cesari et al. (1982) establish a peak force limit of 10 kN for lateral impacts directed at the greater trochanter, and along the axis of the femoral neck. This is the best suited criteria given the information available from the EEVC UL impactor sensors.

Assessment of the proposed modifications to the EEVC UL Protocol

The proposed modifications to the EEVC UL test protocol were employed in simulated EEVC testing of several automotive geometries. The fifteen simplified car geometries used in this study were tested using the Madymo® FE model of the EEVC UL impactor. The simulation results from the modified protocol were then compared to those of the original protocol, as well as against the results from the THUMS FE model and PMTO results.

Generally, the modified EEVC protocol methods employed substantially lower impact velocities than those prescribed by the original version of the EEVC UL testing protocol. This is due a more appropriate characterization of the leading edge and contact velocity between the thigh and the hood.

The proposed modifications to the EEVC test conditions greatly improved correlation to both the THUMS pedestrian model and PMTO impact results for bending moments (Figure 16). However, the modified EEVC simulations still predict higher bending moments than the THUMS simulations or PMTO tests.

A separate test condition (11.1 kg impact mass instead of 7.5 kg) and failure criterion (10kN peak impact force) were applied to those vehicles with an Mod-EEVC LEH greater than 90 cm. Thus, the Van000 geometry and all SUV geometries except SUV500, were tested for pelvic impact. As can be seen in Figure 17, the 10 kN peak impactor force threshold yielded a good correlation with THUMS injury prediction. However, the modified EEVC protocol simulation predicts that a van geometry with no leading edge radius (Van000) will cause no pelvic fracture, while the THUMS model and PMTO experiments predict that this geometry will cause a pelvic fracture to occur. The modified EEVC test

protocol also inherently assumes that no pelvic fracture will occur in vehicles with Mod-EEVC LEH < 90 cm.

Thus the SUV000 and Van050 geometries, for which THUMS simulations predicted pelvic fracture and for the latter of which PMTO tests showed pelvic fracture, were not tested for pelvic injury risk according to the modified EEVC proposal. As indicated by the PMTO test results, it may therefore be necessary to apply both force and bending moment injury criteria to vehicles with LEH near the pelvis/femur decision threshold.
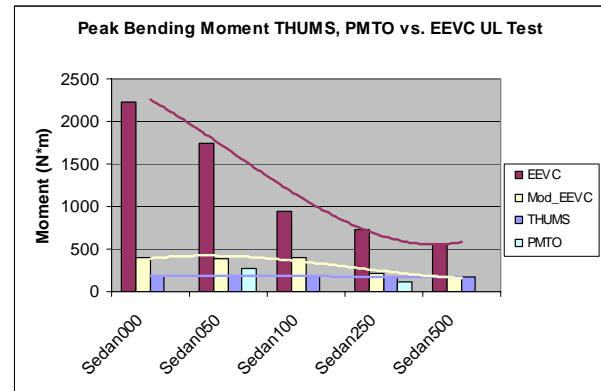
Figure 16. Comparison of the peak bending moments for impact against sedan geometries.
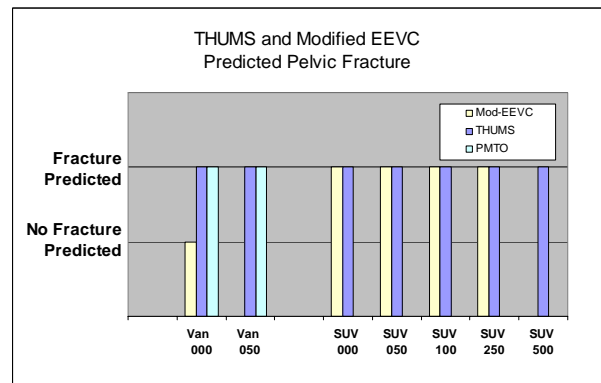
Figure 17. Comparison of pelvic fracture predictions between the modified EEVC protocol, PMTO test results, and the THUMS model.

DISCUSSION

The intelligent design of automotive front-end geometry holds a large potential for reducing injuries to vulnerable road users. In order to assess the risk posed to a pedestrian by an automobile, the European Enhanced Vehicle-Safety Committee has proposed three subsystem pedestrian dummy tests. These tests

are currently in use on production vehicles, and are published regularly by EuroNCAP. For such tests to be useful, it is necessary to concentrate on the most important aspects of automotive design, and employ testing protocols that are capable of successfully identifying high-risk vehicles. The current study focuses on the upper leg impact portion of the EEVC protocol, which is intended to assess the risk presented to the thigh and pelvis of a struck pedestrian.

Vehicle front end design, including hood leading edge height, bumper height, and bumper lead play a critical part in determining the complicated kinematics of pelvic/upper leg contact with the hood leading edge. The EEVC test conditions, which have been based on kinematic analysis of PMTO and dummy impact experiments, intend to incorporate these kinematics into the UL testing protocol. However, the reduction of a complicated three dimensional impact into a simplified, one dimensional impact test appears to fall short in replicating the complex nature of actual upper leg/pelvic impacts (Konosu et al., 2001, Okamoto et al. 2001, Snedeker et al. 2003).

In the current study, a full body FE model, THUMS, was used to simulate pedestrian impact against several simplified automotive geometries. The results from these simulations indicate that hood leading edge radius is an important factor in determining the injury risk posed to a pedestrian by a given automotive form. The model also indicates that acceleration of the distal femur by the bumper and rolling motion imparted to the thigh by the hood radius drastically reduce the closing speed of contact in appropriately designed vehicles. In a previous study we have shown that the current EEVC WG17 upper-leg testing protocol does not reflect these critical factors (Snedeker et al., 2003). The purpose of the present study was to validate the THUMS model predictions against actual PMTO experiments, use the PMTO experiments to deepen our understanding of femur and pelvic injury mechanisms, and use this insight to make recommendations for an improved characterization of vehicle geometry.

In general, the predictive capacity of the THUMS pedestrian model was excellent. The predicted femoral bone strains and bending moments corresponded very well to the experimental PMTO measurements. The model tends to over-estimate the "first-peak" bending moment imparted to the thigh by contact with the bumper. This may imply that the model knee is more rigid than that of the PMTO, in which the soft tissues of the knee dissipate impact energy, and force transmission from the lower leg to the femur is dampened. It may also be due, in part, to the fact that the THUMS model does not account for soft tissue injuries or fracture of the tibia or fibula. Such injuries were observed in three of the five trials, and would serve to inhibit force transmission to the femur.

Interpretation of the strain gauge data from the pubic ramus and femoral neck is more difficult, since the precise loading mechanism of these structures is relatively unknown. These measurements were also complicated by variability in the anatomical placement of the gauges due to individual differences in bone geometry, and difficulty in accessing bone surfaces heavily invested by connective tissue. In an effort to compare the measured bone strain data with the THUMS model, the time history of cortical bone strain was compared against individual finite elements located in corresponding anatomical positions. The element strains in the THUMS pubic rami vary widely between even neighboring elements, suggesting both that the strain distribution in these bone structures is complex and that the mesh discretization was perhaps too coarse. However, the strain time history of certain THUMS elements in each case was similar to that measured with the PMTO strain gauges, and the predicted THUMS stress magnitudes are appropriately matched to the corresponding measurements of PMTO stress magnitude (Figure 11 above).

When considering automotive front end geometry, the observed PMTO injury patterns were surprising. The THUMS model predicted no injuries for any geometry except the van with a sharper hood edge (Van050). It was anticipated that the large bumper lead and hood radius of the sedans, and the van with the rounded hood edge (Van250) would permit sufficient acceleration of the distal femur prior to contact with the hood, such that the closing speed would be reduced and no injury would result. In fact, no injuries to the femur were observed. However, two factors are likely causes to why this hypothesis failed with regard to the pelvis: bone quality and victim stature.

In an attempt to explain the prevalence of pubic rami fracture in PMTOs T2, T4, and T5, test subject bone quality was assessed using pQCT. As can be readily seen in Figure 5, marked differences in bone quality existed between subjects. Further, the three impacts that resulted in pelvic fracture all involved subjects with compromised bone integrity. While these subjects had diminished bone quality with

respect to young healthy adults, their bone quality was typical of the older pedestrians that represent a significant proportion of pedestrian victims. Thus, it appears that age and age-related bone loss may be at least as important as car geometric design when it comes to the injury outcome of a car-pedestrian collision.

Victim stature with respect to leading edge height is the second factor that explains the prevalence of hip and pelvis injuries in these experiments. All THUMS simulations, and indeed most reported biomechanical studies, involve the anatomy of a 50th% man or have data normalized to this standard. Only two of the subjects tested in the present study are representative of such a subject, and the other three subjects were considerably smaller in stature. Thus the hood of a sedan with a leading edge height of 765 mm will most certainly contact a standing 50th% man on the femoral midshaft, but shorter pedestrians are likely to be struck at the hip or pelvis. With regard to PMTOs T1, T2, and T5, the hood front contacted the pedestrian at the hip, and thus these impacts are perhaps better compared to the THUMS being struck by an SUV or van with a high leading edge height. With regard to the hip and pelvic fracture of subject T4, it is possible that the violent loading of the femur due to the sharp hood edge, may have caused a "push-through" fracture of the acetabulum, and a subsequent fracture of the superior ramus.

CONCLUSIONS:

- A method for dynamic measurement of femoral and pelvic bone strains in a laterally struck pedestrian has been successfully established
- The THUMS pedestrian model is capable of accurately assessing pelvic and femoral injury risk in laterally struck pedestrians.
- It may be possible that "safe" cars can be identified using only geometric measurement, and that an UL impactor is unnecessary.
- A car sufficiently exhibiting: low hood leading edge height, large hood edge radius, moderate bumper lead, and high bumper edge height would practically exclude the possibility of a femoral fracture in primary lateral impact of a 50th percentile male pedestrian at impact velocities less than 40 kph.
- Bone quality and pedestrian stature are critical considerations with regard to injury outcome that are not considered by the current EEVC UL test protocol.

- The hood leading edge roundness has an important effect on the upper leg kinematics of pedestrian impact. This effect is not sufficiently encompassed by the one dimensional impactor or the test condition look-up graphs employed in the current version of the EEVC test protocol.
- The closing speed of contact between the thigh and car hood is a critical factor in injury likelihood that does not appear to be sufficiently accounted for in the current EEVC test protocol. The closing speed is often not equivalent to vehicular speed, and can largely depend on the roundedness of the hood leading edge.
- Separate test conditions and test pass/fail criteria should be implemented for low leading edge height (LEH < hip height) and high leading edge height vehicles (LEH > hip height). Specifically, low LEH vehicles should be tested with regard to the femur, and high LEH vehicles should be tested with respect to the pelvis.
- A modified EEVC UL test protocol has been offered. The modified EEVC protocol is based on a logical geometric determination of impact conditions derived from pedestrian anthropometry and vehicle front end shape.
- The modified proposal accounts for reduced impact velocity in cases where the impacted femur has been accelerated by the bumper prior to impact with the hood leading edge thus reducing impact energy.
- The modifications to the EEVC protocol yield impactor bending moments that correspond much better with those predicted by the THUMS pedestrian model and PMTO experiments. It is therefore deemed to be a significant improvement on the current EEVC protocol.
- Validated numerical models provide a powerful low-cost alternative to the use of impactors in assessing pedestrian injury risk.

OUTLOOK

The present study represents a significant leap forward in the assessment of pedestrian injury risk through the use of numerical models. The THUMS pedestrian model has been shown to predict with a high degree of accuracy the resulting pelvic and femoral loading patterns in laterally struck pedestrians. However, there is still work to be done.

The proposed modifications to the EEVC UL test protocol are based upon numerical simulations that require experimental validation. Additionally, the effects of pedestrian stature should be investigated

using numerical models of varying dimensional scale. Finally, the effect of hood stiffness was not addressed in the current work, and a parametric study of hood force-deformation characteristics could provide valuable insight automotive design insight.

ACKNOWLEDGMENTS

REFERENCES

Bunketorp, O., Romanus, B., Hansson, T., Aldman, B., Thorngren, L., Eppinger, R.H. (1983) Experimental study of a compliant bumper system. Proc. 27th Stapp Car Crash Conference, pp. 287-297.

Cesari, D., Ramet, M. (1982) Pelvic tolerance and protection criteria in side impact. Proc. 26th Stapp Car Crash Conference, pp. 145-154.

Cordey J, Gautier E. Strain gauges used in the mechanical testing of bones. Part II: "In vitro" and "in vivo" technique. Injury. 1999;30:A14-20.

EEVC (1998) EEVC-proposal of the EEVC Working Group 17 Report: Improved test methods to evaluate pedestrian protection afforded by passenger cars. Brussels.

Horikoshi T, Endo N, Uchiyama T, Tanizawa T, Takahashi HE. Peripheral quantitative computed tomography of the femoral neck in 60 Japanese women. (1999) Calcif Tissue Int.

Ishikawa, H., Kajzer, J., Schroeder, G. (1993) Computer simulation of impact response of the human body in car-pedestrian accidents. 37th Stapp Car Crash Conference, pp. 235-248.

Iwamoto, M. Kisanuki, Y., Watanabe, I., Furusu, K., Miki, K., Hasegawa, J. (2002) Development of a Finite Element Model of the Total Human Model for Safety (THUMS) and Application to Injury Reconstruction, Proc. 2002 International Research Council on the Biomechanics of Impact (IRCOBI).

Konosu, A., Ishikawa H., Sasaki, A. (1998) A study on pedestrian impact test procedure by computer simulation. In: Proc. 16th International Conference on the Enhanced Safety of Vehicles (ESV).

Konosu A., Ishikawa H., Tanahashi M. (2001) Reconsideration of injury criteria for pedestrian subsystem legform testproblems of rigid legform impactor. In: Proc. of the 17th International Conference on the Enhanced Safety of Vehicles (ESV).

Kress, T A and Porta, D J. (2001) Characterization of Leg Injuries from Motor Vehicle Impacts. In: Proc. of the 17th International Technical Conference on the Enhanced Safety of Vehicles (ESV).

Matsui Y, Ishikawa H, Sasaki A (1998). Validation of Pedestrian Upper Legform Impact Test – Reconstruction of Pedestrian Accidents, Proc. of the 16th International Technical Conference on the Enhanced Safety of Vehicles (ESV).

Matsui Y, Ishikawa H, Sasaki A. (1999) Pedestrian injuries induced by the bonnet leading edge in current car-pedestrian accidents. SAE International Congress and Exposition, Society of Automotive Engineers, Warrendale, Pennsylvania, USA.

McElhaney J.H. (1966), Dynamic Response of Bone and Muscle Tissue. Journal of Applied Physiology, 21, pp. 1231-1236.

Okamoto, Y., Akiyama, A., Okamoto, M., Kikuchi, Y. (2001) A study of the upper leg component tests compared with pedestrian dummy tests. In: Proc. of the 17th International Technical Conference on the Enhanced Safety of Vehicles (ESV).

Powell, W. R., Odala, S. J., Advani, S. H., and Martin, R. B. (1975) Cadaver Femur Responses to Longitudinal Impacts. SAE 751160, Proceedings of the Nineteenth Stapp Car Crash Conference.

Roebuck, J.A., Kroemer, K.H.E., Thomson, W.G. (1975) Engineering Anthropometry Methods. Wiley, New York

Sheppard, C.(2001) "Pelvic Fractures", eMedicine Journal , (www.emedicine.com) 2:6.

Sabotta J., (1993) Sobotta, Atlas der Anatomie des Menschen Band 2. Urban & Fischer.

Snedeker J.G., Muser M.H., Walz F.: Assessment of pelvis and upper leg injury risk in car-pedestrian collisions: Comparison of accident statistics, impactor tests and a human body finite element model. STAPP Car Crash Journal 2003; 47:437-457.

TNO Corporation (2001) Madymo V6.0 Database Manual, Delft, Netherlands

Yamada H. (1971) Strength of Biologic Materials. Krieger, Huntingdon.